Atmospheric Environment 299 (2023) 119658

Contents lists available at ScienceDirect

Atmospheric Environment

journal homepage: www.elsevier.com/locate/atmosenv

Spatial variability and temporal changes of POPs in European background air

Helene Lunder Halvorsen [a,b,*], Pernilla Bohlin-Nizzetto [a], Sabine Eckhardt [a], Alexey Gusev [c], Claudia Moeckel [a,d], Victor Shatalov [c], Lovise Pedersen Skogeng [a], Knut Breivik [a,b]

[a] NILU - Norwegian Institute for Air Research, P.O. Box 100, 2027, Kjeller, Norway
[b] Centre for Biogeochemistry in the Anthropocene, Department of Chemistry, University of Oslo, 0351, Oslo, Norway
[c] Meteorological Synthesizing Centre-East, 115419, Moscow, Russian Federation
[d] Department of Materials and Environmental Chemistry, Stockholm University, 11418, Stockholm, Sweden

HIGHLIGHTS

- Selected POPs were measured in background air across 101 sites in Europe.
- The spatial and temporal variability of POPs across Europe was assessed.
- Mechanistic modelling provided complementary information on source contributions.

GRAPHICAL ABSTRACT

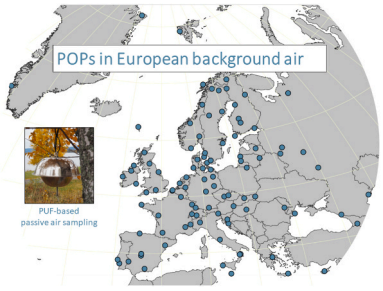

ARTICLE INFO

Keywords:
POPs
Passive air sampling
Atmospheric transport modelling
Spatial variability
Temporal trends
Europe
Primary emissions
Secondary emissions

ABSTRACT

Concentration data on POPs in air is necessary to assess the effectiveness of international regulations aiming to reduce the emissions of persistent organic pollutants (POPs) into the environment. POPs in European background air are continuously monitored using active- and passive air sampling techniques at a limited number of atmospheric monitoring stations. As a result of the low spatial resolution of such continuous monitoring, there is limited understanding of the main sources controlling the atmospheric burdens of POPs across Europe. The key objectives of this study were to measure the spatial and temporal variability of concentrations of POPs in background air with a high spatial resolution (n = 101) across 33 countries within Europe, and to use observations and models in concert to assess if the measured concentrations are mainly governed by secondary emissions or continuing primary emissions. Hexachlorobenzene (HCB) was not only the POP detected in highest concentrations (median: 67 pg/m^3), but also the only POP that had significantly increased over the last decade. HCB was also the only POP that was positively correlated to latitude. For the other targeted POPs, the highest concentrations were observed in the southern part of Europe, and a declining temporal trend was observed. Spatial differences in temporal changes were observed. For example, γ-HCH (hexachlorocyclohexane) had the largest decrease in the south of Europe, while α-HCH had declined the most in central-east Europe. High occurrence of degradation products of the organochlorine pesticides and isomeric ratios indicated past usage. Model predictions of PCB-153 (2,2',4,4',5,5'-hexachlorobiphenyl) by the Global EMEP Multi-media Modelling

* Corresponding author. NILU - Norwegian Institute for Air Research, P.O. Box 100, 2027, Kjeller, Norway.
E-mail address: hlu@nilu.no (H. Lunder Halvorsen).

https://doi.org/10.1016/j.atmosenv.2023.119658
Received 28 October 2022; Received in revised form 23 January 2023; Accepted 13 February 2023
Available online 14 February 2023

System suggest that secondary emissions are more important than primary emissions in controlling atmospheric burdens, and that the relative importance of primary emissions are more influential in southern Europe compared to northern Europe. Our study highlights the major advantages of combining high spatial resolution observations with mechanistic modelling approaches to provide insights on the relative importance of primary- and secondary emission sources in Europe. Such knowledge is considered vital for policy makers aiming to assess the potential for further emission reduction strategies of legacy POPs.

1. Introduction

Persistent organic pollutants (POPs) are regulated organic chemicals that may cause harmful health- and environmental effects, due to their toxicity and bioaccumulating properties. They are persistent and can be transported over long distances, far away from their sources. The atmosphere represents an important pathway of environmental transport across national boundaries and into remote areas (Wania and Mackay, 1993).

Though international regulations have reduced the primary emissions of POPs into the environment, POPs are still present both in source regions and remote regions like the Arctic (Wong et al., 2021). The occurrence of POPs in the atmosphere and other environmental compartments may in part be due to continuing primary emissions (Breivik et al., 2004; UNEP, 2020). However, the relative importance of secondary sources from historically contaminated surface media (Jones, 1994; Li and Wania, 2018) is excpected to increase, due to the decrease in primary emissions (Nizzetto et al., 2010) and/or increased global temperatures (Ma et al., 2011). Monitoring of POPs in air is therefore important to identify the main sources controlling the atmospheric burdens, and to assess the effectiveness of control measures for legacy POPs (Wöhrnschimmel et al., 2016).

POPs have been included in the air monitoring programme of EMEP (the European Monitoring and Evaluation Programme) since 1999 (Tørseth et al., 2012). In 2016, 12 atmospheric monitoring stations in Europe, utilizing active air sampling (AAS) techniques, reported concentrations of POPs in background air to EMEP (Aas and Bohlin-Nizzetto, 2018). These samplers, driven by pumps, provide data with high temporal resolution, but are costly and thereby result in low spatial coverage. The continous monitoring under EMEP is crucial for time-trend analysis at individual sites, but the analysis of spatial variability in Europe is hampered by a low number of EMEP sites and chemical analysis performed by different laboratories. Passive air samplers (PAS) based on diffusive uptake, are independent of electricity and represent a simple and low-cost alternative. PAS may complement AAS by expanding the spatial coverage of air measurement assessments (Jaward et al., 2004; Shoeib and Harner, 2002), such as the EMEP programme. Within Europe, two PAS monitoring networks (Kalina et al., 2019; Schuster et al., 2021) and a few case-studies (Gioia et al., 2007; Halse et al., 2011; Jaward et al., 2004) have contributed to assess the spatial trends, but except Halse et al. (2011) ($n = 86$), the number of sampling sites in background areas within Europe has been limited ($n < 46$). Therefore, a need exists for studies aiming to improve the understanding of the spatial patterns of POPs in European air, as the source contributions are known to be variable across Europe, e.g. due to differences in production and use from country to country. In more central parts of Europe, the production and use of POPs have been widespread (Barber et al., 2005; Breivik et al., 1999, 2002), and we therefore expect the influence of primary emissions to be higher in this region, compared to remote areas in Europe (Jaward et al., 2004; Lunder Halvorsen et al., 2021; Meijer et al., 2003). Furthermore, it is also known that there are major spatial differences in the historical use of legacy POPs within Europe. A notable example is the insecticide lindane (>99% g-HCH) which was used more extensively in western parts of Europe, whereas the historical use of technical HCH (predominantly a-HCH) mainly occurred in eastern parts of Europe (Breivik et al., 1999). We therefore hypothesize that the concentrations of POPs in air within Europe may be a) variable across regions, b) variable for different POPs (both on a group level and for individual compounds), c) likely to have decreased over time in response to primary emission reductions, and d) increasingly influenced by secondary emissions.

The main objective of this study was to assess the spatial and temporal variability of legacy POPs in air across Europe, using a combination of measurements and modelling, both with high resolution. In this study, a comprehensive passive air sampling campaign with 101 sites across Europe was conducted in 2016, mapping background concentrations of POPs in air. The analysis of all PAS was performed by one laboratory, providing a consistent dataset. The study focuses on legacy POPs, that have seen significant historical use in the study region, and enables us to assess the spatial distribution of POPs in European air and their temporal change in concentrations by comparing with studies carried out in the past, including data from a similar PAS campaign conducted in 2006 (Halse et al., 2011). Lunder Halvorsen et al. (2021) recently proposed a strategy on how to combine high spatial resolution measurements with modelling approaches to better understand the main sources controlling atmospheric burdens of POPs across a nation. In our study, the approach was expanded to the whole of Europe.

2. Materials and methods

2.1. Sampling

Passive air samples were collected at 101 background sites across 33 countries within Europe (35°N to 82°N, 52°W to 48°E, Figure SI-1.1) in a coordinated and comprehensive sampling campaign during summer 2016. Most of the sites ($n = 96$) were monitoring stations reporting various inorganic and organic compounds in air to EMEP (see e.g. Tørseth et al. (2012)). Among these, 11 sites (Figure SI-1.1) reported some of the targeted POPs based on AAS to EMEP in 2016 (Aas and Bohlin-Nizzetto, 2018). Passive air samplers were deployed and collected by trained personnel already involved in the EMEP program (Table SI-3.1), following standard operating procedures for passive air sampling of POPs.

Polyurethane foam based passive air samplers (PUF-PAS) with the MONET design of the sampler housing (diameter upper and lower bowl 30 and 24 cm respectively) were used for sampling (Kalina et al., 2017; Markovic et al., 2015). The PUF disks (14 cm diameter x 1.4 cm thickness, 0.027 g/cm^3) were purchased from Sunde Skumplast AS/Carpenter (Norway). Prior to deployment, the PUF disks were pre-cleaned, spiked with sampling performance reference compounds (PRCs, Table 1.2a) and distributed to the sampling sites by NILU. The PUF-PAS were deployed at or close-by the monitoring stations and exposed from July to October (77–125 days). Details of sampler preparation and deployment are described in Lunder Halvorsen et al. (2021) while an overview of the sampling sites is presented in the Supporting Information (Table SI-1.1).

2.2. Sample extraction and clean-up

The exposed PUF disks were returned to the laboratory at NILU for analysis. A description of sample extraction and clean-up is given in SI 1.2.

2.3. Instrumental analysis

Prior to instrumental analysis, an instrument performance standard was added to the samples. The samples were analyzed for 31 polychlorinated biphenyls (PCBs), penta- and hexachlorobenzene (PeCB/HCB) and 27 organochlorine pesticides (OCPs). This included the six indicator PCBs (PCB-28, -52, −101, −138, −153 and −180), hexachlorocyclohexanes (HCHs), dichlorodiphenyldichloroethylenes (DDTs), chlordanes (CDs), aldrin, endosulfans, and their metabolites. A list of all target compounds is given in Table SI-1.2b-c. Analysis was performed with a gas chromatograph (GC) coupled to a high-resolution mass spectrometer (HRMS) following the method described in Lunder Halvorsen et al. (2021).

2.4. QA/QC

Blank level control was performed by extracting and analyzing 14 method blank samples and 11 field blank samples in the same way as the exposed samples. The method detection limits (MDLs) were calculated as the average plus three times the standard deviation of target analytes in blank samples, normalized by the average sample volume (Table SI-2.1b). While the levels in field- and method blanks for the OCPs were comparable and were all used to calculate the MDL, only the method blanks were used to calculate the MDL for PCB and PeCB/HCB. Of the 60 targeted analytes, only analytes with more than 60% detection frequency, i.e. 30 PCBs, PeCB/HCB and 16 OCPs, were evaluated in this study. The median concentrations of these analytes exceeded the MDLs by a factor of 6–111. For the calculation of sum, average and median, and for the statistical analysis, concentrations below MDL were replaced by ½ MDL, for consistency with Halse et al. (2011). There are uncertainties related to the statistical interpretation of data when substituting values below MDL, especially for analytes with less than 85% detection frequency (Helsel, 2006).

The internal standard recoveries of deployed samples, field- and method blanks are given in Table SI-1.3. For further method quality control, a known amount of ^{12}C target analytes was added to three clean PUF disks to assess the method bias (−2%-6% for PCBs and −13%-27% for OCPs, Table SI-1.4a). PUF-PAS were co-deployed at 11 selected sites to assess the reproducibility of the PAS method (0–33 RSD%, Table SI-1.4b).

2.5. Deriving air concentrations

Air concentrations were derived from the amounts found in the samplers and air volumes estimated from the template of Harner (2017), with the same approach described in Lunder Halvorsen et al. (2021). A detailed description of the required parameters is included in SI section 1.3. In short, site-specific sampling rates (2.0–15 m^3/day, median: 3.7 m^3/day, Table SI-1.5) were estimated accounting for i) the measured loss of PRCs from the PUF-PAS, and ii) site-specific environmental conditions, i.e. ambient air temperature (−13-29 °C) and wind speed (2–7 m/s). The median sampling rate in our study is within the range often reported for PUF-PAS (3–4 m^3/day) (Wania and Shunthirasingham, 2020).

The PCBs and OCPs targeted in our study are predominantly in gas-phase (Bohlin et al., 2014), and the lower uptake efficiency for particles with the MONET sampler (Bohlin et al., 2014; Markovic et al., 2015) is therefore not taken into consideration when estimating air volumes. For more volatile compounds with $K_{OA} < 10^8$ (e.g. HCB and PCB-18), equilibrium is reached during the 3-month deployment period (Francisco et al., 2017). The Harner-template accounts for this and the estimated air volumes of HCB are consequently lower than e.g. PCB-153 (Table SI-1.5). However, the PAS does not provide a true time-averaged concentration as the rate of uptake is decreasing during the sampling period. The amount of HCB in the PUF that is in equilibrium with the atmosphere may also change. (Wania and Shunthirasingham, 2020).

2.6. Data analysis

The ratio between maximum and minimum concentrations in air (MMR) was used as a simple measure of the spatial variability. For comparison with the Norwegian study (Lunder Halvorsen et al., 2021), MMR was calculated excluding outliers (SI 1.4.1).

Regional differences in the measured concentrations of POPs between north, south, central-east and west (Figure SI-1.1), according to the geographical division of Europe by the European Union (EuroVoc, 2021), were assessed using significance tests. The spatial variability was further assessed by examining possible correlations between the target compounds, with latitude/longitude as well as with population density estimated within 50 km of each sampling site (SI 1.4.2). All data, except latitude/longitude were log-transformed prior to the correlation tests.

Significance tests were also performed to assess the temporal change in concentrations between this study and an earlier European campaign from 2006 (Halse et al., 2011), for 73 sites that were included in both studies. A consistent comparison to the earlier campaign was assured by using similar sampling and analytical methods, and the same approach for deriving air concentrations accounting for the temperature dependence of $K_{PUF\text{-}air}$.

All statistical analyses were performed by using R Studio with R 4.1.1 (details in SI 1.4).

2.7. Source-receptor modelling tools

Model simulations of concentration of PCB-153 in air were carried out for each individual site, corresponding to the actual deployment periods, using the GLEMOS model (Malanichev et al., 2004). The results were initially used to evaluate if the observed spatial pattern is explained by the model. For each site, the relative contributions attributed to primary- and secondary emissions were predicted by GLEMOS. While the total primary emissions are separated into contributions from national emissions and transboundary transport (within/outside EMEP), this is not specified for the secondary emissions. A correlation between the predicted contribution from national emissions and population density (within 50 km of each site, SI 1.4.2) was examined. Furthermore, regional differences in the relative contribution of the main sources were examined, by using significance tests.

To further examine the source regions and contributions from primary emissions alone, simulations of PCB-153 were also carried out using the Lagrangian particle dispersion model FLEXPART V10.4 in backward mode (Pisso et al., 2019; Stohl et al., 1998). FLEXPART predicts so-called “footprints” that illustrate where the air mass had the potential to take up pollutants from sources near the ground. Combining the footprints with emission data (Breivik et al., 2007) enables us to identify the primary source regions contributing to the predicted concentration at each sampling site.

We refer to Lunder Halvorsen et al. (2021) for further details on the model simulations that were carried out.

3. Results and discussion

3.1. Overall results

An overview of concentrations in air, detection frequencies (i.e. percentage of samples above MDL) and MMRs of selected POPs in air is provided in Table SI-2.1a, while concentrations for all target analytes at the individual sites are presented in Tables SI-2.2a-b. The median concentration of $\sum_{30}$PCBs was 29 pg/m^3 (range: 3–405 pg/m^3), and 30 of the 31 targeted PCB congeners were detected in more than 60% of the samples. The six indicator PCBs (45% of $\sum_{30}$PCBs), PCB-18 (11%), PCB-31 (8%), and PCB-149 (8%) were most abundant. The concentrations of $\sum_6$PCBs (median: 13 pg/m^3, range: 1–241 pg/m^3) were comparable to

previously reported passive air data from European background sites in the Global Atmospheric Passive Sampling (GAPS) network (n = 11, 5 coinciding with our study) between 2011 and 2014 (median $\sum_7$PCBs: 12 pg/m^3) (Schuster et al., 2021). The median ratio between PAS concentrations of $\sum_6$PCB in our study and AAS concentrations reported to EMEP (Aas and Bohlin-Nizzetto, 2018) for the same sites (n = 10) and sampling period, was 1.8 (PAS/AAS-ratio: 0.4–9.6, Figure SI-1.3a), which is within the uncertainty of PAS and AAS in combination (Holt et al., 2017).

The highest concentrations were measured for HCB (median: 67 pg/m^3) and PeCB (median: 25 pg/m^3). Of the 27 targeted OCPs, 16 were detected in more than 88% of the samples (Table SI-2.1a). The other 11 OCPs were only detected in <60% of the samples with median concentrations ≤0.7 pg/m^3. α- and γ-HCHs were detected in highest amounts (median: 9 pg/m^3), followed by *p,p'*-DDE, dieldrin and endosulfan I (medians: 6, 4 and 3 pg/m^3, respectively). On average, *p,p'*-DDE accounted for 58% of the sum of all six targeted DDTs (median $\sum_6$DDXs: 10 pg/m^3), while *p,p'*-DDT and *o,p'*-DDT accounted for 18% and 14% respectively. Heptachlor-exo-epoxide, a degradation product of Heptachlor, was detected in all samples, with concentrations (median: 2 pg/m^3) similar to the concentrations of the sum of four chlordanes (Table SI-2.1a, median $\sum_4$chlordanes: 2 pg/m^3). Of the chlordanes, cis-chlordane and trans-nonachlor were dominating (41% and 38% of median $\sum_4$chlordanes respectively). The oxygenated metabolite of chlordanes, oxy-chlordane, was found in similar concentrations to trans-nonachlor and cis-chlordane (median: 1 pg/m^3).

The median concentrations of HCHs, Dieldrin, cis-chlordane and trans-nonachlor in this study were within a factor of two of the concentrations from PAS deployed at European background sites in the study of Schuster et al. (2021). However, the median concentration of endosulfan I in our study was a factor of five lower than in the study by Schuster et al. (2021) (16 pg/m^3). This may be explained by the steeper declining rate of endosulfan I compared to other compounds, as a consequence of later phase-out (i.e. 2011) and higher environmental degradation rate (Schuster et al., 2021). The concentrations of HCB, HCHs, $\sum_3$DDXs (*p,p'*-DDD/-DDE/-DDT) and Dieldrin using PAS in our study were on average 2.4 times higher (PAS/AAS-ratio: 1.0–23) than the concentrations from AAS reported to EMEP (n = 11) for the same sites and time period (Figures SI-1.3 b-f) (Aas and Bohlin-Nizzetto, 2018). Differences between studies may be caused by analytical uncertainties (due to e.g. different chemical laboratories) and uncertainty in the estimated sampling volumes (due to sampling artifacts or environmental conditions not being fully accounted for in the calculations, SI-1.3.1). A direct comparison to EMEP is further affected by differences in sampling methodology, including differences in AAS strategies within the EMEP program.

3.2. Spatial variability

The spatial variability of $\sum_6$PCBs in Europe, when excluding outliers (MMR in this study = 60) (SI 1.4.1), is considerably larger than in Norway (MMR~4) (Lunder Halvorsen et al., 2021). The lowest concentrations of $\sum_6$PCBs (<5 pg/m^3) were generally found in northern Europe (e.g. Norway, Sweden, Finland) and on the British Isles (west region) (Figure SI-2.2a). The correlation analysis (Table SI-2.4) further showed a significant north-south gradient for PCBs ($r = -0.46$, $p < 0.001$), whereby the median concentration within the south region (13 pg/m^3, Table SI-2.3) was twice as high as in the north (6.5 pg/m^3, $p = 0.008$). The larger spatial variability within Europe compared to Norway, together with the observed north-south gradient, implies that the atmospheric concentrations of PCBs at southern latitudes in Europe may be influenced by primary emissions of PCBs to a larger extent than at northern latitudes (Breivik et al., 2007; Jaward et al., 2004). The low levels of PCBs on the British Isles may be explained by the prevailing wind regimes with transport of air masses arriving from the Atlantic Ocean, as shown by the map of footprint emission sensitivities for PCB-153 (e.g. Yarner Wood, site 92, UK, Figure SI-2.3).

Hotspots (outliers >60 pg/m^3) for PCBs were Abastumani (site 29, Georgia) and Zmeiny Island (site 88, Ukraine) in the central-east region (241 and 100 pg/m^3), Ayia Marina (site 7, Cyprus) in the south region (90 pg/m^3), Keldsnor (site 11, Denmark), Risoe (site 13, Denmark) and Nuuk (site 40, Greenland) in the north region (73, 70 and 66 pg/m^3), and De Zilk (site 60, the Netherlands, 70 pg/m^3) in the west region. Significantly elevated concentrations of PCBs at a specific site may indicate influence from local sources and imply that the site may not be representative for background concentrations in that area. Examples of sources resulting in possible local influence may be populated areas (e.g. Nuuk, Greenland), forest fires (e.g Ayia Marina, Cyprus) (San-Miguel-Ayanz et al., 2017) and PCB contaminated building materials, equipment etc. in the vicinity of the sampler (e.g. Keldsnor, Denmark) (Halse et al., 2011). However, such possible local influences are less likely when several sites in the same area are consistently high (e.g. the Netherlands, 52–70 pg/m^3, n = 3).

The lowest spatial variabilities were found for HCB (and PeCB) (MMR = 15 and 6). HCB has previously been shown to be evenly distributed across Europe (Jaward et al., 2004) and the globe (Shunthirasingham et al., 2010) explained by the long residence time of HCB in the atmosphere (Beyer et al., 2003). Elevated concentrations at e.g. Rucava (site 52, Latvia, 413 pg/m^3) may however implicate that emissions of HCB are still ongoing in the vicinity of some sites (Fig. 1a). This has also been suggested by Hung et al. (2016).

Interestingly, HCB was the only POP in our study that was significantly positively correlated to latitude ($r = 0.44$, $p < 0.001$, Table SI-2.4). After Rucava (Latvia), the highest concentrations were observed at the Arctic sites; Station Nord (site 41, Greenland, 247 pg/m^3) and Zeppelin (site 96, Spitsbergen, 130 pg/m^3). As HCB has reached equilibrium between the PUF and air well within the sampling period at all sites, the sample volumes for this compound are largely depended on $K_{PUF\text{-}air}$ (Francisco et al., 2017). Consequently, the low temperatures at Zeppelin (Spitsbergen) and Station Nord (Greenland) (4 °C and −13 °C respectively, Table SI-1.5) resulted in sample air volumes (355 m^3 and 297 m^3) in the upper range of the other sites (average 217 m^3, Table SI-1.5). When comparing the concentrations at these sites with concentrations from the co-located AAS reported to EMEP (Figures SI-1.3b) (Aas and Bohlin-Nizzetto, 2018), the PAS/AAS-ratio was 1.6 and 3.3 respectively. These ratios are within the expected range (2–3) (Holt et al., 2017) and hence reflect that the environmental conditions have been compensated for in the estimation of sampling volumes. Enhanced re-emissions from previously contaminated surface reservoirs (Ma et al., 2011) and increasing primary emissions have been put forward as possible explanations (Platt et al., 2022) for the higher concentrations of HCB in the Arctic compared to central Europe. Model predictions in the latter study suggested that Arctic haze periods with high concentrations of HCB in air in the Norwegian Arctic were associated with transport of contaminated air masses from Asia. When excluding the three above-mentioned sites, there is still a significant positive correlation with latitude ($r = 0.37$, $p < 0.001$), suggesting generally higher concentrations of HCB in northern Europe, not only in the Arctic.

Similar to PCBs, a north-south gradient ($r < 0$, Table SI-2.4) was also observed for the OCPs, though not statistically significant for all. One example is the HCHs, for which only γ-HCH was significantly negatively correlated to latitude ($r = -0.55$, $p < 0.001$), while a minor correlation was found for α-HCH ($r = -0.14$, $p = 0.15$). The spatial variability for γ-HCH (2–109 pg/m^3, MMR = 55) was also larger compared to α-HCH (4–47 pg/m^3, MMR = 12). These differences may reflect the higher LRAT potential of α-HCH compared to γ-HCH (Beyer et al., 2003), but also that Lindane (>99% γ-HCH) was exempted from the SC for use in the control of head lice and scabies (UNEP, 2020), and hence used more recently than technical HCH (55–80% α-HCH, 8–15% γ-HCH (Breivik et al., 1999)). The HCHs were furthermore correlated to longitude; the highest concentrations of α-HCH (Figure SI-2.4a) were observed in the

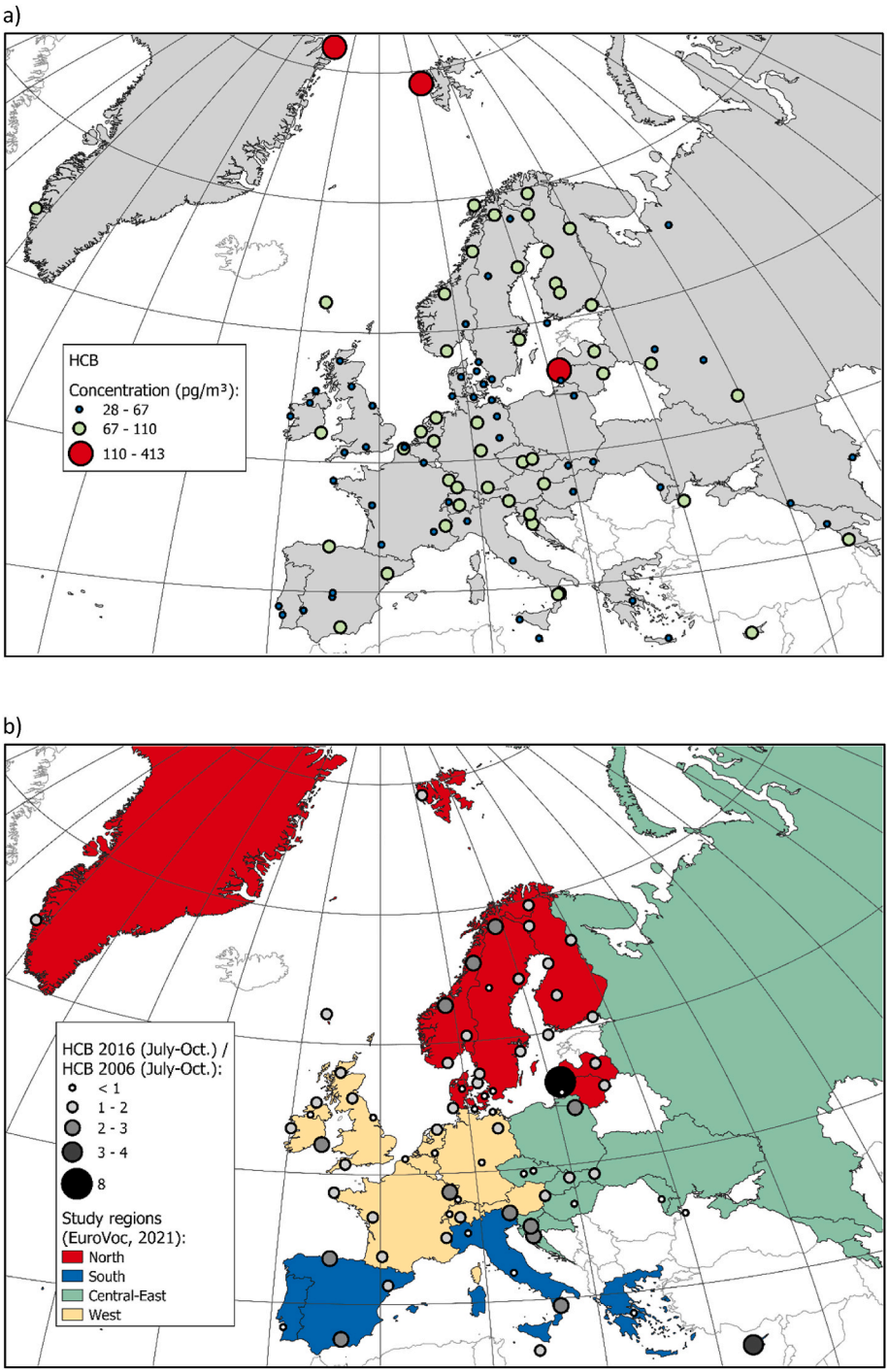

Fig. 1. (a) Concentrations of HCB in air across Europe (n = 101, this study), and (b) measured concentrations of HCB in 2016 (this study) divided by measured concentrations of HCB in 2006 (Halse et al., 2011) at European sites for which data for both years are available (n = 73).

central-east region (median: 18 pg/m^3), while the highest concentrations of γ-HCH (Figure SI-2.4b) were observed in the west region (median: 27 pg/m^3). This may reflect the later phase-out and large stockpiles of pesticides in the central-east region (e.g. Moldova and Ukraine) (Pribylova et al., 2012), and that Lindane was extensively used in e.g. France in the west region (Breivik et al., 1999; Vijgen et al., 2019).

The $\sum_6$DDXs (Figure SI-2.5) showed the largest variability in Europe (0.3–286 pg/m^3, MMR $\sum_6$DDX >953) of the targeted compounds. The variability of e.g. *p,p'*-DDT (MMR~433) was substantially larger in Europe, compared to Norway (MMR~15) (Lunder Halvorsen et al., 2021). This suggests that some European sites may be influenced by continuing primary sources. The most significant difference ($p < 0.001$) between the south- and the north region were also found for $\sum_6$DDXs (south/north-ratio 6.5, Table SI-2.3), reflecting that the LRAT potential is less than for the more volatile HCB and HCHs (Shen et al., 2005), but also the continued use of DDT (UNEP, 2020). Like α-HCH, a west-east gradient was observed for $\sum_6$DDXs, with highest median concentration of $\sum_6$DDXs in the central-east region (35 pg/m^3), approximately four times higher than the west region (9.2 pg/m^3). High concentrations of $\sum_6$DDX were measured at sites in e.g. Ukraine, Moldova and the Czech Republic (146–286 pg/m^3), in line with previous findings (Halse

et al., 2011; Pribylova et al., 2012).

Similar to $\sum_6$DDXs, significantly ($p < 0.001$) higher concentrations were observed for endosulfan I in the south region than in the north region (south/north-ratio 4.6, Table SI-2.3), with the proximity to primary sources in the south region as a possible explanation. Though elevated concentrations of endosulfan I (16–21 pg/m^3, Figure SI-2.6) were measured in Armenia (site 1, Amberd) and Georgia (site 29, Abastumani) in the central-east region, endosulfan I was not significantly correlated to longitude. The very high concentrations of endosulfan I at Iskrba (site 72, Slovenia, 82 pg/m^3) may be an indication of local contribution.

The correlation analysis between the target POPs (Table SI-2.4) appears to reflect some similarities in the spatial patterns of emission sources. The positive correlation between all targeted POPs (except HCB) is likely to be a result of consistently higher concentrations in southern Europe compared to northern Europe. Furthermore, the positive correlation with estimated population density (within 50 km of the sampling sites) observed for all POPs (except HCB and α-HCH), suggests that high concentrations of most POPs can largely be attributed to elevated emissions occurring in the most populated areas in Europe.

The strongest correlation ($0.84 < r < 0.95$) was found between dieldrin (<MDL-37 pg/m^3), $\sum_4$chlordanes (0.5–35 pg/m^3), heptachlor-exo-epoxide (0.4–63 pg/m^3) and oxy-chlordane (<MDL-9 pg/m^3). These OCPs also have similar spatial patterns, with highest concentrations measured in the west region (e.g. Netherlands and Belgium, Figures SI-2.7-2.10). The median concentrations of these OCPs in the west region were up to three times higher than the median concentrations in the central-east region (Table SI-2.3). This finding aligns with the results by Halse et al. (2011), who also reported elevated levels of $\sum_4$chlordanes in the Netherlands and Belgium.

3.3. Temporal change

When comparing our results on the basis of median concentrations of all POPs with the 73 common European sites in the study of Halse et al. (2011), only HCB had higher median concentration in 2016 than in 2006 (56% increase, Table SI-2.5). The increase for HCB (i.e. 2016/2006-ratio >1.2) was evident at 68% of the sampling sites (Fig. 1b), while no obvious change (i.e. 2016/2006-ratio: 0.8.-1.2) was observed for the remaining sites. Data from long-term monitoring sites based on AAS shows an inconsistent time-trend in HCB concentrations (Gusev et al., 2015; Ilyin et al., 2022; Kalina et al., 2019; Wong et al., 2021). Of three sites with available AAS-data for both 2006 and 2016 (i.e. Zeppelin, Birkenes and Kosetice), only Zeppelin showed an increase in the HCB concentration with a 2016/2006 ratio of 1.1 (Table SI-2.6), while the ratio was below 1 at the other two sites. In comparison, our PAS results showed an increase at two of the three sites, i.e Birkenes and Zeppelin, with a 2016/2006 ratio of 1.8 and 1.3 respectively. This difference may be explained by that the PAS and AAS have been exposed to different air masses (i.e. time-average of 3 months-vs. daily/weekly-samples).

No clear spatial pattern was observed, but the increase was larger at some specific sites. For example, at Rucava (site 52, Latvia), the concentration of HCB in 2016 was almost eight times higher than in 2006, substantiating possible local contribution at this site in 2016. The increase observed in the Arctic (e.g. site 96, Zeppelin, 2016/2006-ratio: 1.3), is in accordance with the stable or increasing concentrations reported in the Arctic from 1992 to 2018 by Wong et al. (2021).

The concentrations of the other POPs (i.e. PCBs, HCHs, DDXs and chlordanes) have decreased significantly ($p < 0.05$) between 2006 and 2016 (Table SI-2.5), i.e. −28% decrease in the median concentrations for $\sum_6$PCBs, −59% for α-HCHs, −48% for γ-HCHs, −12% for $\sum_4$DDXs (*p,p'*-DDD/-DDE/-DDT, *o,p'*-DDT) and −23% for $\sum_4$chlordanes. For both $\sum_4$DDXs and $\sum_4$chlordanes, a significant decrease was only observed in the west region (−45% and −27% respectively). This is consistent with the overall decreasing trend reported for these POPs at AAS sites within EMEP (Gusev et al., 2015; Hung et al., 2016; Kalina et al., 2019). While there were small differences in the median concentrations of $\sum_4$chlordanes between the four regions, in both 2006 (2.2–3.7 pg/m^3) and 2016 (2.0–3.1 pg/m^3), $\sum_4$DDXs were substantially higher for the central-east region (77 pg/m^3 in 2006 and 61 pg/m^3 in 2016), compared to the other regions (Figure SI-2.11 c).

It should be noted that the detection frequencies of the DDXs were higher in 2016 than in 2006. This may be explained by a lower method detection limit in 2016. For example, the MDL for *p,p'*-DDE was 0.18 pg/m^3 in 2016 while 1.6 pg/m^3 in 2006, and consequently *p,p'*-DDE was detected in all samples in 2016, while only in 74% of the samples in 2006. When disregarding the 20 sites where the concentration of *p,p'*-DDE in 2006 was below MDL, a decrease in the median concentration of *p,p'*-DDE for the remaining 53 sites was still observed (Figure SI-2.12), but it was not statistically significant ($p = 0.084$). As a consequence of lower MDL and the ability to detect lower concentrations in 2016, the variability of *p,p'*-DDE was substantially larger in our study (MMR 1017) when considering all sites, than reported by both Halse et al. (2011) (MMR>177) and Jaward et al. (2004) (MMR>29).

For PCBs, the largest decrease in median concentrations was observed in the north- and central-east regions (−48% and −35%), followed by the west region (−22%). On the other hand, the median concentration of $\sum_6$PCBs in the south region in 2016 were comparable to 2006. The MMR of $\sum_6$PCBs in 2016 is 211 when including all sites, which is higher than previously reported for the background sites in the European studies of Schuster et al. (2021) (MMR $\sum_7$PCBs = 58, n = 11) and Jaward et al. (2004) (MMR $\sum_6$PCBs >24, n = 46). A smaller difference in MMRs is observed when comparing only with the common sites (n = 73) in the study of Halse et al. (2011) (MMR 45 in 2006 and MMR 88 in 2016). The high MMR when including all sites in 2016 may therefore likely reflect the larger spatial coverage across Europe in our study compared to previous studies, which illustrates the benefits of high spatial resolution.

α-HCH was found at highest concentrations in the central-east region in both 2016 (median 17 pg/m^3) and in 2006 (median 55 pg/m^3), but the median concentration has decreased substantially (−69%). In the north region, the decrease of α-HCH was smaller than in the other regions (−22%) (Figure SI-2.11 a-d). This may be explained by the northern sites being more influenced by climate change and thereby from increased re-volatilization from sea and ice melting (Halse et al., 2012; Ma et al., 2011; Shen et al., 2004), compared to the other regions in Europe. For γ-HCH, the decrease was substantially higher for the south- (−76%), central-east- (−56%) and west region (−45%), compared to the north region (−21%). Consequently, the south/north-ratio (of medians) was reduced from 6.7 in 2006 to 2.0 in 2016. The largest decrease for α-HCH and γ-HCH is observed in the historical primary source regions were technical HCH and Lindane have been more extensively used, respectively (Breivik et al., 1999), and reflect that the immediate effect on air concentrations from emissions reductions is larger in source areas, compared to more remote areas.

3.4. Source indications

A higher proportion of the more chlorinated PCBs is expected closer to source regions, as heavier PCBs tend to be less prone to LRAT (Beyer et al., 2003). Accordingly, high relative abundance of PCB-153, compared to PCB-28 (Figure SI-2.13), in combination with elevated measured concentrations, may reveal potential source areas and/or locally affected sites. Consequently, higher PCB-153/PCB-28 ratios were observed in southern Europe than in northern Europe. The highest ratio was observed for Abastumani (site 29, Georgia, PCB-153/PCB-28-ratio: 14, Figure SI-2.13), followed by Keldsnor (site 11, Denmark), Porspoder (site 26, France) and Risoe (site 13, Denmark) (PCB-153/PCB-28-ratios: 3–4). For all these sites (except Porspoder), the high ratios are accompanied with elevated $\sum_6$PCB concentrations (i.e. outliers >70 pg/m^3, Figure SI-2.2a), substantiating that sources may exist in the vicinity.

The α-/γ–HCH–ratios in this study (range: 0.1–7.7, Figure SI-2.14) and within EMEP (range: 0.2–41 (Aas and Bohlin-Nizzetto, 2018),) were highest in northern Europe (correlation with latitude in this study; $r = 0.53$, $p < 0.001$), suggesting that LRAT and/or re-volatilization of α-HCH are important in this region (Halse et al., 2012; Shen and Wania, 2005). The lower α-/γ–HCH–ratios in southern Europe may further reflect the vicinity to countries which have experienced significant historical use and emissions of γ-HCH (Breivik et al., 1999). For example, the α-/γ–HCH–ratio at Waldhof (site 35, Germany) were 0.3 in this study and 0.2 within EMEP respectively.

Isomeric ratios can be used to assess whether more "weathered" isomers are dominating, and hence indicate possible shifts from primary-to secondary sources (Becker et al., 2012; Pozo et al., 2006). One example is the DDXs, for which a weathered signal with the ratio (*p,p'*-DDE + *p,p'*-DDD)/*p,p'*-DDT larger than 1.3 was found at 92% of the sites (Figure SI-2.15a), indicating past usage of technical DDT in Europe. (Li and Macdonald, 2005; Ricking and Schwarzbauer, 2012). A weathered signal of *p,p'*-DDT in European air was also shown in 2006 (Halse et al., 2011). When comparing the ratio for the 53 sites above MDL in 2006 with the ratio in 2016, 17 sites had a lower ratio in 2016 (Figure SI-2.15b). For Montelibretti (site 47) and Ispra (site 46) in Italy, the ratios decreased from 2.8 to 1.5 and 2.6 to 1.5 respectively. As the *p,p'*-DDT concentration at the site had increased, while there was no reduction in the *p,p'*-DDE concentration, the observed decrease may be a result of possible influence from primary emissions of *p,p'*-DDT.

Several countries in Europe (e.g. Spain, Italy and Turkey) have utilized dicofol in agriculture (Denier van der Gon et al., 2007). Dicofol is synthesized from DDT (Qiu et al., 2005) and has shown to have a higher content of the *o,p'*-DDT isomer compared to technical DDT. In our study, 29% of the sites had *o,p'*-DDT/*p,p'*-DDT ratios between 1.0 and 3.2 (Figure SI-2.15c), and influence from dicofol may therefore be expected. However, elevated ratios up to 14 have previously been reported in areas where dicofol is suspected to be the dominant source (Ricking and Schwarzbauer, 2012). The highest ratios in our study were found in northern Europe (including Svalbard with ratio 3.2), which instead may be explained by differences in the LRAT potential of the two isomers due to a greater vapour pressure of the *o,p'*-DDT isomer (Spencer and Cliath, 1972). Preferential mobilization of the *o,p'*-DDT isomer from soil to air (Ricking and Schwarzbauer, 2012) may also explain the elevated ratios at some of the sites in our study.

The expected proportion of trans- and cis-chlordane from technical chlordane in ambient air is 1.6 (Jantunen et al., 2000). Due to greater reactivity of trans-chlordane compared to cis-chlordane in the environment (Becker et al., 2012; Bidleman et al., 2002), the low trans-/cis-chlordane ratio observed in our study (median 0.27, less than 1.6 at 99% of the sites) may indicate that the occurrence of chlordanes in European atmosphere is mostly influenced by historical use. This is further supported by the high detection frequency of oxy-chlordane (99%), which is a metabolite of the chlordanes. Houtem (site 4) in Belgium, with the highest concentration of $\sum_4$chlordanes (35 pg/m^3), also shows a high ratio of trans-/cis-chlordane (2.2, Figure SI-2.16), which implicates possible influence from more recent use of technical chlordane in the vicinity of the site.

Technical chlordane also contains 7% of heptachlor (Dearth and Hites, 1991). The dominance of the degradation product heptachlor-exo-epoxide (detected at all sites) in our study, compared to heptachlor (7% detected frequency), could therefore indicate past usage of technical chlordane in Europe, but could also be due to past usage of technical heptachlor (Bidleman et al., 2002). It should be noted that heptachlor was detected with highest concentration in the sample from Houtem (21 pg/m^3, 32 times the MDL). This substantiates possible fresh usage of one of these pesticides at the site (Hung et al., 2002).

While aldrin was not detected in any of the samples, dieldrin was detected in 98% of the samples. Aldrin is degraded to dieldrin in the environment (Gannon and Bigger, 1958), and the high abundance of dieldrin may therefore implicate re-volatilization of either dieldrin and/or aldrin.

The technical mixture of endosulfan consists of >95% of the endosulfan I and –II, in ratios between 2:1 and 7:3 (Weber et al., 2010). While endosulfan I was detected at all sites, the detection frequency of endosulfan II was only 45%. This may be explained by the higher content of endosulfan I in the technical mixture and that endosulfan II may be converted to endosulfan I in the environment (Schmidt et al., 1997; Weber et al., 2010). The high median endosulfan I/endosulfan II-ratio (8.5) across Europe may further suggest high degree of conversion of endosulfan II, and hence implicates previous use of endosulfan. In contrast, the low ratios at Iskrba (site 72, Slovenia, ratio: 1.4) and Capo Granitola (site 50, Spain, ratio: 2.4) (Figure SI-2.17), accompanied with the highest measured concentrations of both endosulfan I (82 and 24 pg/m^3) and endosulfan-II (58 and 9.9 pg/m^3), suggest more recent use at these sites. It is also noteworthy that the detection frequency of endosulfan II is higher compared to the detection frequency in the Norwegian study (5% only) (Lunder Halvorsen et al., 2021), which may be a result of endosulfan II being washed out more easily during atmospheric transport (Shen et al., 2005).

3.5. Model predictions of PCB-153

Concentrations of PCB-153 in air predicted by GLEMOS and FLEXPART were within a factor of three of the observed concentrations for 62% and 65% of the sampling sites respectively. Both models generally underestimated the measured concentrations, i.e. the ratio of measured/predicted concentrations was larger than one for 81% of the sites with GLEMOS and 84% of the sites with FLEXPART. The highest deviations were found in the north and east regions (Figure SI-2.18). The underestimation observed for both FLEXPART and GLEMOS may in part be due to uncertainties in the emission data used as input to the models (Lunder Halvorsen et al., 2021). Secondly, FLEXPART ignores secondary emissions, hence lower predicted concentrations with FLEXPART are expected. However, FLEXPART predicted lower concentrations only at 45% of the sites and the FLEXPART/GLEMOS ratio ranged from 0.3 to 3.0. Thirdly, there are also uncertainties related to the estimated atmospheric loss during transport with the two models. A comparison of predicted and observed concentrations (Figure SI-2.18), may help identifying sites or areas where emissions are either under- or overestimated. The most noticeable example is Abastumani (site 29, Georgia) where the highest measured concentration of PCB-153 (78 pg/m^3) was found in this study. The measured concentration at this site far exceeds what both GLEMOS (0.45 pg/m^3) and FLEXPART (0.31 pg/m^3) predict. When excluding the concentration measured at Abastumani, the spatial variabilities of PCB-153 obtained from the two models (MMR = 566 for GLEMOS, MMR = 229 for FLEXPART), are larger than the observed spatial variability (MMR = 161) in the study region. The underestimation with GLEMOS is largest when low concentrations are predicted (e.g. in the north region, Figure SI-2.18), resulting in a possible overestimated MMR.

GLEMOS (Table SI-2.7) predicts that secondary emissions are, on average, four times more important (median 78%) than total primary emissions (i.e. national emissions and transboundary transport within/outside EMEP) in controlling atmospheric burdens. The contributions from secondary emissions (Fig. 2) are predicted to be largest at sites in Russia and Finland (92–95%, e.g. Pinega, site 64, Figure SI-2.19a). The footprint map of Pinega, obtained from FLEXPART (Figure SI-2.19b), shows low input of primary emissions from other areas.

According to GLEMOS, the contributions from total primary emissions (Fig. 2) to the measured concentrations on the sites varied from 5% to 61% (median 22%), with the exception of Station Nord at Greenland (site 41, 94%). Significantly larger (p-value<0.001) contribution from primary emissions in the south and west region (median 35% and 28% respectively), compared to the north and central-east region (median 18% and 16% respectively) were observed. National primary emissions (Fig. 2) were predicted to contribute 0–53% (median 11%) to the

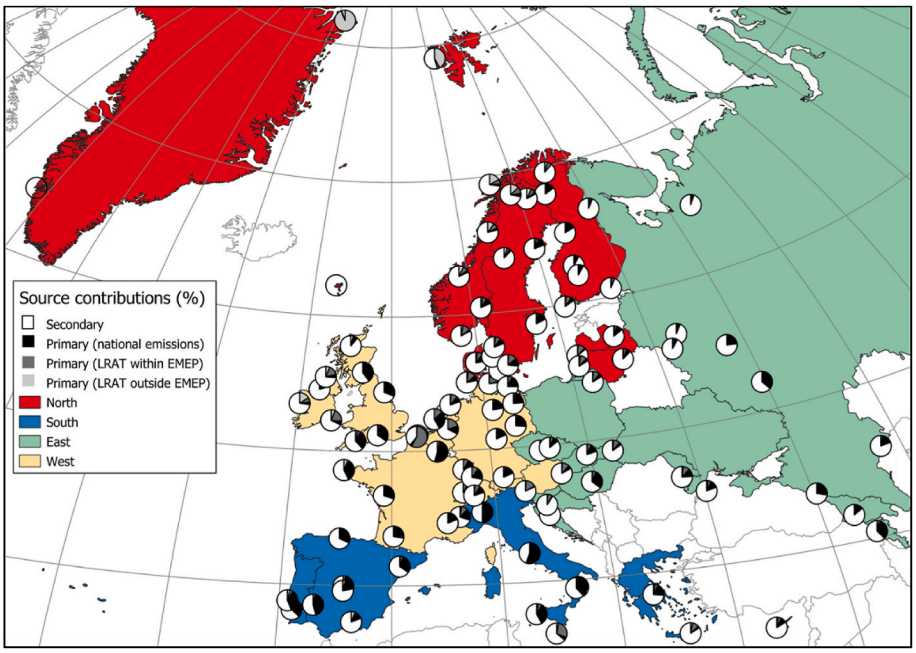

Fig. 2. Predicted relative contribution of secondary and primary emissions of PCB-153 attributed to national emissions and transboundary transport from countries within/outside EMEP, predicted by The Global EMEP Multi-media Modeling System (GLEMOS). The different study regions are indicated in the background map.

concentrations of PCB-153 and followed a similar spatial pattern as the total primary emissions. Barcarotta in Spain (site 78, south region, Figure SI-2.20a) is an example of a site that is predicted to be highly influenced by national emissions (41%). The footprint map (Figure SI-2.20b), showing largest input in the vicinity to the sampling site, also reflects this.

It should be noted that many of the selected background sites are not necessarily designated sites for the measurement of PCBs, but rather background sites for other air quality indicators. Both the observed concentrations of PCB-153 and the predicted total primary emissions correlated significantly (p-values <0.001) with the estimated population density within 50 km radius of the sampling site ($r = 0.63$ and $r = 0.51$). The highest densities (690–2700 persons per km^2) were found for nine sampling sites which had a city within this region (red circles in Figure SI-1.8), and it may therefore be questioned if these are representative background sites in the measurement of PCBs. For example, Alfragide (site 63, Portugal) was located in the immediate vicinity of Lisbon city. Not surprisingly, the observed concentrations of PCB-153 for these "suburban" sites (3.3–17 pg/m^3) were found to be significantly higher ($p < 0.001$) than all other sites (median 1.8 pg/m^3, <610 habitants/km^2). This "suburban effect" was largely captured by GLEMOS, which predicted the influence from national emissions to be significantly higher (p-value = 0.01) for the "suburban" sites (5–53%), compared to the other sites (median 11%).

On the other hand, the influence from transboundary transport within/outside EMEP (Fig. 2) were 5% and 2% (medians) respectively, and were predicted to be largest in the north region (median 9%). This is in line with the findings in our Norwegian study (Lunder Halvorsen et al., 2021), in which 15% was attributed to LRAT. Both Station Nord (site 41, Greenland) and Zeppelin (site 96, Spitsbergen) in the north region were predicted to be highly influenced by primary sources outside EMEP (93% and 42% respectively), compared to the other sites (<17%). This was also demonstrated in the footprint map for Zeppelin (Lunder Halvorsen et al., 2021). Malanichev et al. (2004) has further shown that American emission sources are one of the main contributors to the atmospheric concentrations of PCB-153 in the Arctic in summer. In contrast, e.g. Houtem (site 4, Belgium) had the largest predicted influence from transboundary transport within EMEP (58%), predominantly from France (56%) (Figure SI-2.21a). The footprint map (Figure SI-2.21b) further showed high emission contributions beyond the nation's boundaries, within the EMEP region. The EMEP countries that contributed most frequently to the atmospheric burdens of PCB-153 at sites in other countries, were France (67%), Germany (48%), UK (38%), Belgium (18%), Italy (18%), Russia (17%), Spain (16%), Sweden (16%), Finland (11%), Netherlands (10%), Denmark (10%) and Ukraine (9%). However, these numerical values are affected by the geographical location and density of sites, as well as the predominant air flow across Europe (west to east). For example, as the number of sites is relatively large east of the French border, a relatively large number of sites are likely to have been influenced by emissions in France.

4. Conclusions

In this extensive spatial mapping study, HCB and HCHs were found to dominate the atmospheric background concentrations of POPs across Europe. The highest spatial variability, on the other hand, was found for $\sum_6$DDXs (MMR>953) and $\sum_6$PCB (MMR = 240). For most POPs, higher concentrations were observed in southern Europe than in northern Europe, reflecting the proximity to historical source regions. In contrast, the concentrations of HCB increased with latitude. The elevated concentrations of HCB observed in the Arctic may be explained by enhanced influence of re-volatilization, but primary emissions of HCB have also been suggested to be influential (Platt et al., 2022).

HCB was the only POP with higher concentrations in 2016 than in 2006. An increase was observed at 68% of the sites, distributed across Europe, with an increase of 56% in the median concentration of HCB from 2006 to 2016. High concentrations of HCB due to pesticide use have previously been reported in central parts of Europe (Barber et al., 2005), and enhanced influence of secondary emissions from previously contaminated soil may be possible. However, the increase in concentrations of HCB in air could also be a consequence of an increase in primary emissions. This highlights the need for further studies separating the contributions from primary and secondary sources of HCB, and future source-receptor modelling studies should therefore target HCB. The increased concentrations also imply that further monitoring of HCB is needed.

On the other hand, the observed decline in the median atmospheric concentrations from 2006 to 2016 for α-HCH (−59%), γ-HCH (−48%), $\sum_6$PCBs (−28%), $\sum_4$chlordanes (−23%) and $\sum_4$DDXs (−12%) reflects that the primary emissions in the study region have declined. The largest decreases are observed in historical primary source regions while the smallest decreases are observed in remote regions which are more influenced by secondary emissions and/or long-range atmospheric transport from outside Europe. For the PCBs, no significant decrease and a higher proportion of the more chlorinated PCB-153 than PCB-28 was observed in the south region, implying more influence of primary sources in this region. This was supported by model predictions of PCB-153 using GLEMOS that showed that the contribution from secondary emissions is, on average, four times higher than primary emissions in most of the study area while primary emissions of PCB-153 are more influential at southern latitudes.

For $\sum_6$DDXs and $\sum_4$chlordanes, the decrease was only significant in the west region. Isomeric ratios for OCPs showed that most sites are influenced by secondary sources from historical usage of pesticides. For DDXs, however, the isomeric ratio indicates that some sites may be influenced by primary emissions of technical DDT. Furthermore, the spatial patterns of the dominating isomers suggest that the influence of secondary sources was largest at southern latitudes in Europe. Secondary emissions from applications of technical aldrin, -chlordane and -heptachlor were more dominating in the west region than the east region.

Implications of continued influence of primary emissions of PCBs and DDXs in some regions, suggest that these compounds should be prioritized in future monitoring of POPs. Within EMEP, the MMRs based on active air sampling concentrations were 11 for $\sum_6$PCB (n = 10) and 328 for sum of p,p'-DDD/DDE/DDT (n = 11). This is substantially lower than the spatial variability (240 and 1135 respectively) based on all sites in our study (n = 101) and suggests that the spatial variability of PCBs and DDXs in Europe is not fully captured by the ongoing monitoring activities within EMEP.

Our study highlights the advantages of combining high spatial resolution observations with mechanistic modelling approaches as an important supplement to ongoing long-term monitoring efforts at EMEP sites. As this study offers results which provide new insights on the relative importance of primary and secondary emission sources on a European scale, it thereby also offers knowledge which can be used by policy makers to assess potential opportunities for further emission reductions of legacy POPs. While this study has focused on selected legacy POPs only, the strategy of combining high resolution monitoring and modelling can be expanded towards a wider range of semi-volatile organic chemicals in the future. However, due to the lower uptake efficiency for particles with our MONET-sampler (Markovic et al., 2015), alternative sampling strategies will ideally be required if targeting trace-levels of particle-associated chemicals.

CRediT authorship contribution statement

Helene Lunder Halvorsen: Methodology, Validation, Formal analysis, Investigation, Writing – original draft, Project administration, Visualization. **Pernilla Bohlin-Nizzetto:** Methodology, Investigation, Validation, Writing – review & editing, Supervision. **Sabine Eckhardt:** Formal analysis, Writing – review & editing, Visualization. **Alexey Gusev:** Formal analysis, Visualization. **Claudia Moeckel:** Validation, Formal analysis, Investigation, Writing – review & editing, Visualization. **Victor Shatalov:** Formal analysis, Visualization. **Lovise Pedersen Skogeng:** Investigation. **Knut Breivik:** Conceptualization, Validation, Writing – review & editing, Supervision, Project administration, Funding acquisition.

Declaration of competing interest

The authors declare that they have no known competing financial interests or personal relationships that could have appeared to influence the work reported in this paper.

Data availability

Data will be made available on request.

Acknowledgements

The authors thank numerous volunteers within the EMEP programme for their valuable assistance in the field, and colleagues at NILU for support. This study received financial support from the Research Council of Norway (244298 and 287114) and EMEP.

Appendix A. Supplementary data

Supplementary data to this article can be found online at https://doi.org/10.1016/j.atmosenv.2023.119658.

References

Aas, W., Bohlin-Nizzetto, P., 2018. Heavy Metals and POP Measurements, 2016. EMEP/CCC-Report 3/2018). Kjeller: NILU Retrieved from. http://hdl.handle.net/11250/2563390.

Barber, J.L., Sweetman, A.J., van Wijk, D., Jones, K.C., 2005. Hexachlorobenzene in the global environment: emissions, levels, distribution, trends and processes. Sci. Total Environ. 349 (1), 1–44. https://doi.org/10.1016/j.scitotenv.2005.03.014.

Becker, S., Halsall, C.J., Tych, W., Kallenborn, R., Schlabach, M., Manø, S., 2012. Changing sources and environmental factors reduce the rates of decline of organochlorine pesticides in the Arctic atmosphere. Atmos. Chem. Phys. 12 (9), 4033–4044. https://doi.org/10.5194/acp-12-4033-2012.

Beyer, A., Wania, F., Gouin, T., Mackay, D., Matthies, M., 2003. Temperature dependence of the characteristic travel distance. Environ. Sci.Technol. 37 (4), 766–771. https://doi.org/10.1021/es025717w.

Bidleman, T.F., Jantunen, L.M.M., Helm, P.A., Brorström-Lundén, E., Juntto, S., 2002. Chlordane enantiomers and temporal trends of chlordane isomers in arctic air. Environ. Sci.Technol. 36 (4), 539–544. https://doi.org/10.1021/es011142b.

Bohlin, P., Audy, O., Škrdlíková, L., Kukučka, P., Přibylová, P., Prokeš, R., Vojta, Š., Klánová, J., 2014. Outdoor passive air monitoring of semi volatile organic compounds (SVOCs): a critical evaluation of performance and limitations of polyurethane foam (PUF) disks. Environ. Sci. J. Integr. Environ. Res.: Process. Impacts 16 (3), 433–444. https://doi.org/10.1039/C3EM00644A.

Breivik, K., Pacyna, J.M., Münch, J., 1999. Use of α-, β- and γ-hexachlorocyclohexane in Europe, 1970–1996. Sci. Total Environ. 239 (1–3), 151–163. https://doi.org/10.1016/s0048-9697(99)00291-0.

Breivik, K., Sweetman, A., Pacyna, J.M., Jones, K.C., 2002. Towards a global historical emission inventory for selected PCB congeners–a mass balance approach. 2. Emissions. Sci. Total Environ. 290 (1–3), 199–224. https://doi.org/10.1016/s0048-9697(01)01076-2.

Breivik, K., Alcock, R., Li, Y.F., Bailey, R.E., Fiedler, H., Pacyna, J.M., 2004. Primary sources of selected POPs: regional and global scale emission inventories. Environ. Pollut. 128 (1–2), 3–16. https://doi.org/10.1016/j.envpol.2003.08.031.

Breivik, K., Sweetman, A., Pacyna, J.M., Jones, K.C., 2007. Towards a global historical emission inventory for selected PCB congeners - a mass balance approach-3. An update. Sci. Total Environ. 377 (2–3), 296–307. https://doi.org/10.1016/j.scitotenv.2007.02.026.

Dearth, M.A., Hites, R.A., 1991. Complete analysis of technical chlordane using negative ionization mass spectrometry. Environ. Sci.Technol. 25 (2), 245–254. https://doi.org/10.1021/es00014a005.

Denier van der Gon, H., van het Bolscher, M., Visschedijk, A., Zandveld, P., 2007. Emissions of persistent organic pollutants and eight candidate POPs from UNECE–Europe in 2000, 2010 and 2020 and the emission reduction resulting from the implementation of the UNECE POP protocol. Atmos. Environ. 41 (40), 9245–9261. https://doi.org/10.1016/j.atmosenv.2007.06.055.

EuroVoc, 2021. Browse by EuroVoc. Retrieved from. https://eur-lex.europa.eu/browse/eurovoc.html. Access Dec 2021.

Francisco, A.P., Harner, T., Eng, A., 2017. Measurement of polyurethane foam – air partition coefficients for semivolatile organic compounds as a function of temperature: application to passive air sampler monitoring. Chemosphere 174, 638–642. https://doi.org/10.1016/j.chemosphere.2017.01.135.

Gannon, N., Bigger, J.H., 1958. The conversion of aldrin and heptachlor to their epoxides in Soil1. J. Econ. Entomol. 51 (1), 1–2. https://doi.org/10.1093/jee/51.1.1.

Gioia, R., Sweetman, A.J., Jones, K.C., 2007. Coupling passive air sampling with emission estimates and chemical fate modeling for persistent organic pollutants (POPs): a feasibility study for northern Europe. Environ. Sci.Technol. 41 (7), 2165–2171. https://doi.org/10.1021/es0626739.

Gusev, A., Rozovskaya, O., Shatalov, V., Aas, W., Bohlin-Nizzetto, P., 2015. EMEP Status Report 3/2015. Assessment of Spatial and Temporal Trends of POP Pollution on Regional and Global Scale. Moscow: Meteorological Synthesizing Centre – East Retrieved from. https://www.msceast.org/reports/3_2015.pdf.

Halse, A.K., Schlabach, M., Eckhardt, S., Sweetman, A., Jones, K.C., Breivik, K., 2011. Spatial variability of POPs in European background air. Atmos. Chem. Phys. 11 (4), 1549–1564. https://doi.org/10.5194/acp-11-1549-2011.

Halse, A.K., Schlabach, M., Sweetman, A., Jones, K.C., Breivik, K., 2012. Using passive air samplers to assess local sources versus long range atmospheric transport of POPs. J. Environ. Monit. 14 (10), 2580–2590. https://doi.org/10.1039/c2em30378g.

Harner, T., 2017. 2017_v1_5_Template for Calculating Effective Air Sample Volumes for PUF and SIP Disk Samplers_Sept_15. Retrieved from. https://www.researchgate.net/publication/319764519_2017_v1_5_Template_for_calculating_Effective_Air_Sample_Volumes_for_PUF_and_SIP_Disk_Samplers_Sept_15. Access June 2019.

Helsel, D.R., 2006. Fabricating data: how substituting values for nondetects can ruin results, and what can be done about it. Chemosphere 65 (11), 2434–2439. https://doi.org/10.1016/j.chemosphere.2006.04.051.

Holt, E., Bohlin-Nizzetto, P., Borůvková, J., Harner, T., Kalina, J., Melymuk, L., Klánová, J., 2017. Using long-term air monitoring of semi-volatile organic compounds to evaluate the uncertainty in polyurethane-disk passive sampler-derived air concentrations. Environ. Pollut. 220, 1100–1111. https://doi.org/10.1016/j.envpol.2016.11.030.

Hung, H., Halsall, C.J., Blanchard, P., Li, H.H., Fellin, P., Stern, G., Rosenberg, B., 2002. Temporal trends of organochlorine pesticides in the Canadian arctic atmosphere. Environ. Sci.Technol. 36 (5), 862–868. https://doi.org/10.1021/es011204y.

Hung, H., Katsoyiannis, A.A., Brorstrom-Lunden, E., Olafsdottir, K., Aas, W., Breivik, K., Bohlin-Nizzetto, P., Sigurdsson, A., Hakola, H., Bossi, R., Skov, H., Sverko, E., Barresi, E., Fellin, P., Wilson, S., 2016. Temporal trends of persistent organic pollutants (POPs) in arctic air: 20 years of monitoring under the arctic monitoring and assessment programme (AMAP). Environ. Pollut. 217, 52–61. https://doi.org/10.1016/j.envpol.2016.01.079.

Ilyin, I., Batrakova, N., Gusev, A., Kleimenov, M., Rozovskaya, O., Shatalov, V., Strizhkina, I., Travnikov, O., Vulykh, N., Breivik, K., Bohlin-Nizzetto, P., Pfaffhuber, K.A., Aas, W., Poupa, S., Wankmueller, R., Ullrich, B., Bank, M., Ho, Q.T., Vivanco, M.G., Theobald, M.R., Garrido, J.L., Gil, V., Couvidat, F., Collette, A., Mircea, M., Adani, M., Delia, I., Kouznetsov, R.D., Kadancev, E.V., 2022 (Status Report 2/2022). Assessment of Heavy Metal and POP Pollution on Global, Regional and National Scales. Moscow: Meteorological Synthesizing Centre - East Retrieved from. https://www.msceast.org/reports/2_2022.pdf.

Jantunen, L.M.M., Bidleman, T.F., Harner, T., Parkhurst, W.J., 2000. Toxaphene, chlordane, and other organochlorine pesticides in Alabama air. Environ. Sci. Technol. 34 (24), 5097–5105. https://doi.org/10.1021/es001197y.

Jaward, F.M., Farrar, N.J., Harner, T., Sweetman, A.J., Jones, K.C., 2004. Passive air sampling of PCBs, PBDEs, and organochlorine pesticides across Europe. Environ. Sci. Technol. 38 (1), 34–41. https://doi.org/10.1021/es034705n.

Jones, K., 1994. Observations on long-term air-soil exchange of organic contaminants. Environ. Sci. Pollut. Control Ser. 1, 172. https://doi.org/10.1007/BF02986940.

Kalina, J., Scheringer, M., Borůvková, J., Kukučka, P., Přibylová, P., Bohlin-Nizzetto, P., Klánová, J., 2017. Passive air samplers as a tool for assessing long-term trends in atmospheric concentrations of semivolatile organic compounds. Environ. Sci. Technol. 51 (12), 7047–7054. https://doi.org/10.1021/acs.est.7b02319.

Kalina, J., White, K.B., Scheringer, M., Přibylová, P., Kukučka, P., Audy, O., Klánová, J., 2019. Comparability of long-term temporal trends of POPs from co-located active and passive air monitoring networks in Europe. Environ. Sci. J. Integr. Environ. Res.: Process. Impacts 21 (7), 1132–1142. https://doi.org/10.1039/C9EM00136K.

Li, Y.F., Macdonald, R.W., 2005. Sources and pathways of selected organochlorine pesticides to the Arctic and the effect of pathway divergence on HCH trends in biota: a review. Sci. Total Environ. 342 (1–3), 87–106. https://doi.org/10.1016/j.scitotenv.2004.12.027.

Li, L., Wania, F., 2018. Occurrence of single- and double-peaked emission profiles of synthetic chemicals. Environ. Sci. Technol. 52 (8), 4684–4693. https://doi.org/10.1021/acs.est.7b06478.

Lunder Halvorsen, H., Bohlin-Nizzetto, P., Eckhardt, S., Gusev, A., Krogseth, I.S., Moeckel, C., Shatalov, V., Skogeng, L.P., Breivik, K., 2021. Main sources controlling atmospheric burdens of persistent organic pollutants on a national scale. Ecotoxicol. Environ. Saf. 217, 112172 https://doi.org/10.1016/j.ecoenv.2021.112172.

Ma, J., Hung, H., Tian, C., Kallenborn, R., 2011. Revolatilization of persistent organic pollutants in the Arctic induced by climate change. Nat. Clim. Change 1, 255–260. https://doi.org/10.1038/nclimate1167.

Malanichev, A., Mantseva, E., Shatalov, V., Strukov, B., Vulykh, N., 2004. Numerical evaluation of the PCBs transport over the northern hemisphere. Environ. Pollut. 128 (1), 279–289. https://doi.org/10.1016/j.envpol.2003.08.040.

Markovic, M.Z., Prokop, S., Staebler, R.M., Liggio, J., Harner, T., 2015. Evaluation of the particle infiltration efficiency of three passive samplers and the PS-1 active air sampler. Atmos. Environ. 112, 289–293. https://doi.org/10.1016/j.atmosenv.2015.04.051.

Meijer, S.N., Ockenden, W.A., Steinnes, E., Corrigan, B.P., Jones, K.C., 2003. Spatial and temporal trends of POPs in Norwegian and UK background air: implications for global cycling. Environ. Sci.Technol. 37 (3), 454–461. https://doi.org/10.1021/es025620+.

Nizzetto, L., Macleod, M., Borgå, K., Cabrerizo, A., Dachs, J., Guardo, A.D., Ghirardello, D., Hansen, K.M., Jarvis, A., Lindroth, A., Ludwig, B., Monteith, D., Perlinger, J.A., Scheringer, M., Schwendenmann, L., Semple, K.T., Wick, L.Y., Zhang, G., Jones, K.C., 2010. Past, present, and future controls on levels of persistent organic pollutants in the global environment. Environ. Sci.Technol. 44 (17), 6526–6531. https://doi.org/10.1021/es100178f.

Pisso, I., Sollum, E., Grythe, H., Kristiansen, N.I., Cassiani, M., Eckhardt, S., Arnold, D., Morton, D., Thompson, R.L., Groot Zwaaftink, C.D., Evangeliou, N., Sodemann, H., Haimberger, L., Henne, S., Brunner, D., Burkhart, J.F., Fouilloux, A., Brioude, J., Philipp, A., Seibert, P., Stohl, A., 2019. The Lagrangian particle dispersion model FLEXPART version 10.4. Geosci. Model Dev. (GMD) 12 (12), 4955–4997. https://doi.org/10.5194/gmd-12-4955-2019.

Platt, S.M., Hov, Ø., Berg, T., Breivik, K., Eckhardt, S., Eleftheriadis, K., Evangeliou, N., Fiebig, M., Fisher, R., Hansen, G., Hansson, H.C., Heintzenberg, J., Hermansen, O., Heslin-Rees, D., Holmén, K., Hudson, S., Kallenborn, R., Krejci, R., Krognes, T., Larssen, S., Lowry, D., Lund Myhre, C., Lunder, C., Nisbet, E., Nizzetto, P.B., Park, K. T., Pedersen, C.A., Aspmo Pfaffhuber, K., Röckmann, T., Schmidbauer, N., Solberg, S., Stohl, A., Ström, J., Svendby, T., Tunved, P., Tørnkvist, K., van der Veen, C., Vratolis, S., Yoon, Y.J., Yttri, K.E., Zieger, P., Aas, W., Tørseth, K., 2022. Atmospheric composition in the European arctic and 30 years of the Zeppelin observatory, ny-Ålesund. Atmos. Chem. Phys. 22 (5), 3321–3369. https://doi.org/10.5194/acp-22-3321-2022.

Pozo, K., Harner, T., Wania, F., Muir, D.C.G., Jones, K.C., Barrie, L.A., 2006. Toward a global network for persistent organic pollutants in air: results from the GAPS study. Environ. Sci.Technol. 40 (16), 4867–4873. https://doi.org/10.1021/es060447t.

Pribylova, P., Kares, R., Boruvkova, J., Cupr, P., Prokes, R., Kohoutek, J., Holoubek, I., Klanova, J., 2012. Levels of persistent organic pollutants and polycyclic aromatic hydrocarbons in ambient air of Central and Eastern Europe. Atmos. Pollut. Res. 3 (4), 494–505. https://doi.org/10.5094/APR.2012.057.

Qiu, X., Zhu, T., Yao, B., Hu, J., Hu, S., 2005. Contribution of dicofol to the current DDT pollution in China. Environ. Sci.Technol. 39 (12), 4385–4390. https://doi.org/10.1021/es050342a.

Ricking, M., Schwarzbauer, J., 2012. DDT isomers and metabolites in the environment: an overview. Environ. Chem. Lett. 10 (4), 317–323. https://doi.org/10.1007/s10311-012-0358-2.

San-Miguel-Ayanz, J., Durrant, T., Boca, R., Libertà, G., Branco, A., De Rigo, D., Ferrari, D., Maianti, P., Vivancos, T., Schulte, E., Loffler, P., 2017. Forest Fires in Europe, Middle East and North Africa 2016. (EUR 28707 EN). Publications Office of the European Union, Luxembourg. Retrieved from. https://data.europa.eu/doi/10.2760/17690.

Schmidt, W.F., Hapeman, C.J., Fettinger, J.C., Rice, C.P., Bilboulian, S., 1997. Structure and asymmetry in the isomeric conversion of β- to α-endosulfan. J. Agric. Food Chem. 45 (4), 1023–1026. https://doi.org/10.1021/jf970020t.

Schuster, J.K., Harner, T., Eng, A., Rauert, C., Su, K., Hornbuckle, K.C., Johnson, C.W., 2021. Tracking POPs in global air from the first 10 Years of the GAPS network (2005 to 2014). Environ. Sci.Technol. 55 (14), 9479–9488. https://doi.org/10.1021/acs.est.1c01705.

Shen, L., Wania, F., 2005. Compilation, evaluation, and selection of Physical−Chemical property data for organochlorine pesticides. J. Chem. Eng. Data 50 (3), 742–768. https://doi.org/10.1021/je049693f.

Shen, L., Wania, F., Lei, Y.D., Teixeira, C., Muir, D.C.G., Bidleman, T.F., 2004. Hexachlorocyclohexanes in the north American atmosphere. Environ. Sci.Technol. 38 (4), 965–975. https://doi.org/10.1021/es034998k.

Shen, L., Wania, F., Lei, Y.D., Teixeira, C., Muir, D.C.G., Bidleman, T.F., 2005. Atmospheric distribution and long-range transport behavior of organochlorine pesticides in north America. Environ. Sci.Technol. 39 (2), 409–420. https://doi.org/10.1021/es049489c.

Shoeib, M., Harner, T., 2002. Characterization and comparison of three passive air samplers for persistent organic pollutants. Environ. Sci.Technol. 36 (19), 4142–4151. https://doi.org/10.1021/es020635t.

Shunthirasingham, C., Oyiliagu, C.E., Cao, X., Gouin, T., Wania, F., Lee, S.-C., Pozo, K., Harner, T., Muir, D.C.G., 2010. Spatial and temporal pattern of pesticides in the global atmosphere. J. Environ. Monit. 12 (9), 1650–1657. https://doi.org/10.1039/C0EM00134A.

Spencer, W.F., Cliath, M.M., 1972. Volatility of DDT and related compounds. J. Agric. Food Chem. 20 (3), 645–649. https://doi.org/10.1021/jf60181a057.

Stohl, A., Hittenberger, M., Wotawa, G., 1998. Validation of the Lagrangian particle dispersion model FLEXPART against large-scale tracer experiment data. Atmos. Environ. 32 (24), 4245–4264. https://doi.org/10.1016/S1352-2310(98)00184-8.

Tørseth, K., Aas, W., Breivik, K., Fjaeraa, A.M., Fiebig, M., Hjellbrekke, A.G., Myhre, C.L., Solberg, S., Yttri, K.E., 2012. Introduction to the European Monitoring and Evaluation Programme (EMEP) and observed atmospheric composition change during 1972-2009. Atmos. Chem. Phys. 12 (12), 5447–5481. https://doi.org/10.5194/acp-12-5447-2012.

UNEP, 2020. Stockholm Convention on Persistent Organic Pollutants (POPs). *Texts and annexes. Revised in 2019.* Switzerland: Secretariat of the Stockholm Convention Retrieved from. http://chm.pops.int/TheConvention/Overview/TextoftheConvention/tabid/2232/Default.aspx.

Vijgen, J., de Borst, B., Weber, R., Stobiecki, T., Forter, M., 2019. HCH and lindane contaminated sites: European and global need for a permanent solution for a long-time neglected issue. Environ. Pollut. 248, 696–705. https://doi.org/10.1016/j.envpol.2019.02.029.

Wania, F., Mackay, D., 1993. Global fractionation and cold condensation of low volatility organochlorine compounds in polar-regions. Ambio 22 (1), 10–18.

Wania, F., Shunthirasingham, C., 2020. Passive air sampling for semi-volatile organic chemicals. Environ. Sci. J. Integr. Environ. Res.: Process. Impacts 22 (10), 1925–2002. https://doi.org/10.1039/D0EM00194E.

Weber, J., Halsall, C.J., Muir, D., Teixeira, C., Small, J., Solomon, K., Hermanson, M., Hung, H., Bidleman, T., 2010. Endosulfan, a global pesticide: a review of its fate in the environment and occurrence in the Arctic. Sci. Total Environ. 408 (15), 2966–2984. https://doi.org/10.1016/j.scitotenv.2009.10.077.

Wöhrnschimmel, H., Scheringer, M., Bogdal, C., Hung, H., Salamova, A., Venier, M., Katsoyiannis, A., Hites, R.A., Hungerbuhler, K., Fiedler, H., 2016. Ten years after entry into force of the Stockholm Convention: what do air monitoring data tell about its effectiveness? Environ. Pollut. 217, 149–158. https://doi.org/10.1016/j.envpol.2016.01.090.

Wong, F., Hung, H., Dryfhout-Clark, H., Aas, W., Bohlin-Nizzetto, P., Breivik, K., Mastromonaco, M.N., Lundén, E.B., Ólafsdóttir, K., Sigurðsson, Á., Vorkamp, K., Bossi, R., Skov, H., Hakola, H., Barresi, E., Sverko, E., Fellin, P., Li, H., Vlasenko, A., Zapevalov, M., Samsonov, D., Wilson, S., 2021. Time trends of persistent organic pollutants (POPs) and Chemicals of Emerging Arctic Concern (CEAC) in Arctic air from 25 years of monitoring. Sci. Total Environ. 775, 145109 https://doi.org/10.1016/j.scitotenv.2021.145109.